

# Exploring the Sensitivity of MiniPix Devices to the Detection of a Variety of Particles

Megan Lawie<sup>1,3,\*</sup>, Freddie Vosper<sup>2,3,\*</sup>, Alexander Booth<sup>3</sup>, Linda Cremonesi<sup>3</sup>

<sup>1</sup> University of Southampton, Department of Physics and Astronomy, Southampton, SO17 1BJ, UK

<sup>2</sup> University of Sussex, Department of Physics and Astronomy, Falmer, Brighton, BN1 9RH, UK

<sup>3</sup> Queen Mary University, Particle Physics Research Centre, London, E1 4NS, UK

\*Corresponding authors (Email: [mrl2g20@soton.ac.uk](mailto:mrl2g20@soton.ac.uk), [fv56@sussex.ac.uk](mailto:fv56@sussex.ac.uk))

## Abstract

The MiniPix EDU devices by ADVACAM have been used to study electrons, muons and alpha particles from both thoriated tungsten rods and natural sources. The natural radiation experiments looked at muons, focusing on the determination of muon count as a function of detector altitude and inclination with respect to the horizon. This included taking readings at ground level compared to those atop a building, and the floors in between, and rotating the detector face a certain angle to find the optimal angle to detect muons. The experiments involving a radiation source looked at alpha and beta decay. This included using the detector's measurement of kinetic energy to explore the relativistic nature of electrons produced via beta decay, and the decay characteristics of alpha radiation. The material attenuation of alpha particles has also been explored. Insights from these experiments provide data on the capabilities of the detector. Through these experiments, particle behaviour and interactions unfold, shedding light on fundamental scientific principles. The project's experiments and results have been simplified to cater to secondary school education, specifically GCSE-level students. The experiments are designed to be performed within a school setting, helping students to understand these fundamental scientific principles of physics.

**Keywords** – Cosmic Ray Muons; Radiation; Particle Detector; MiniPix EDU Detector; ADVACAM

## 1. Introduction

The MiniPix EDU is a device manufactured by ADVACAM [1], designed as a USB “camera” to detect particle radiation for educational use. This technology was designed by the European Organisation for Nuclear Research (CERN) and is used by astronauts at NASA to study radiation in space [2]. Dr Cremonesi and Dr Booth acquired four of these devices through the Queen Mary Centre of Public Engagement (CPE) [3] funding to develop a scientific outreach project through the Physics Research in the School Environment (PRiSE) Scheme [4], with the intent of finding the most applicable, and achievable experiments that can be performed in secondary school classrooms. The detectors themselves have particular hardware and software limitations, which were determined and examined closely. Ultimately, a wide variety of experiments were constructed for the detection of different forms of radiation including alpha, electrons and muons. These experiments included the use of both natural radiation and source radiation from a thoriated rod. The experimental procedures to perform each measurement were closely documented and are described later in this paper.



**Figure 1.** Image of the ADVACAM MiniPix EDU detectors being used in this project.

## 2. Anatomy of the Detector

ADVACAM's imaging technology uses direct conversion single photon counting pixel detectors. The term direct conversion refers to the immediate conversion of radiation into electric charge within the semiconductor crystal. The term single photon counting means that every single particle of radiation detected in an individual pixel is processed

and counted. This property eliminates all other sources of noise that are present in other types of detectors or flat-panel-based cameras. The photon counting “cameras” can directly measure incoming photons’ energy. In the MiniPix detector, the energy deposited by every particle is measured by recording the number of clock cycles that the discriminator output is above the threshold level (this is usually called Time-Over-Threshold).

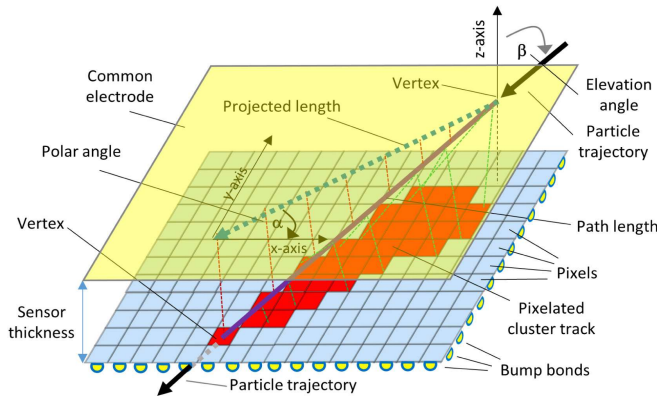


**Figure 2.** Layers of the MiniPix detector. The detector provides an array of  $256 \times 256$  pixels with a total of 65536 independent channels [5].

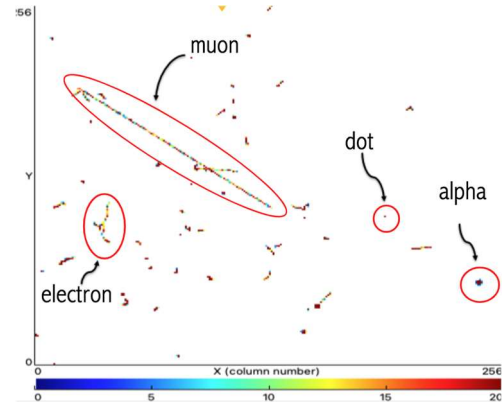


**Figure 3.** Picture of the MiniPix detector software screen used to run the experiments.

Figure 2 shows an example particle going through the minipix, and how it deposits energy in the detector. The MiniPix detector is proficient in detecting and recognising alpha particles, electrons and muons. Alpha particles have a distinct high energy centre, with lower energy on the outside. They appear as a circular blob on the detector screen, with a red centre and a blue outer edge, red denoting a higher energy. Electron tracks are curved paths on the detector screen, usually of a similar colour, where the similar colour of the pixels denotes a similar deposit of energy on each pixel. Muons appear as long, straight tracks on the detector surface, which have a lot more variation in colour. The dots are small amounts of energy, or background radiation, which is deposited onto a few pixels, which could be anything from a photon to a neutrino. Figure 3 shows examples of the different types of particles that can be detected.

The TimePix algorithm [7,8,9] within the Pixet software, is able to recognise the distinct tracks each different particle leaves when it makes contact with the detector and records a count of each. The detector’s ability to accurately count particles in this way is utilised throughout the work described in this paper.

### 3. Experiments

A series of experiments have been conducted in order to understand the detecting capabilities of the MiniPix, consequently illuminating the possible experimental avenues that could be explored. These experiments represent the first step towards designing experiments catered to GCSE students performing them in school. Radiation has been explored in via two avenues, one being naturally occurring radiation, and the other being from a source. Outlined below are some of the experiments that have been conducted, showing their valuable outcomes that help to understand the sensitivity of the detector's capabilities.

#### 3.1 Natural Radiation Experiments

There is an abundance of natural sources of radiation all around us such as the sun, geological formations, structures, and even in food. The experimental focus when studying this type of radiation was to investigate ambient radiation levels, particularly muons originating from cosmic radiation, and to find the best angle at which to detect these muons.

In this project, a particular point of interest for both research and orientation towards secondary schools was the

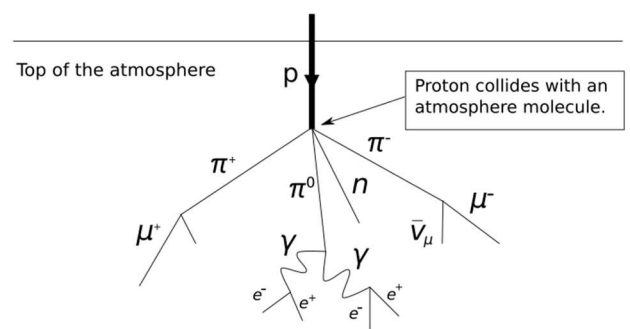


**Figure 4.** An “Air shower”, created from the collision of a cosmic ray proton with a molecule in the atmosphere [6].

nature of cosmic rays. Every second, thousands of cosmic rays, mostly  $H_2$  and He nuclei strike every square metre of the Earth's upper atmosphere. When cosmic rays crash into air molecules in the atmosphere, they create a shower of other particles: pions  $\pi$ , kaons K, positrons  $e^+$ , electrons  $e^-$ , neutrons n, neutrinos  $\nu$ , gammas  $\gamma$  and muons  $\mu$ . As discussed previously, the Pixet software, for the MiniPix EDU detectors, contains algorithms for recognising certain radiation types. One of these types is muons, therefore, the detectors can be used to detect these decayed cosmic rays.

### 3.1.1 Variation in Muon Detection with Changing Altitude

The objective of this investigation was to assess the sensitivity of the MiniPix EDU particle detector across different floors of a building. The experiment aimed to determine whether there is a discernible variation in the number of detected particles based on the floor's elevation. The scale of the study was a range from the scale of tens of metres up to one hundred metres to explore potential sensitivity trends.

Data was collected across multiple floors of the Queen Mary Physics Building. Ensuring uniform conditions, including an equal number of windows in each room, was hugely important. This keeps consistency in the amount of natural radiation entering a room. The collected data was analysed and graphed, as shown in Figure 5.

When a "frame" of data is taken, the detector records the detected energy and particles on the detector screen. The length of time of a frame can be varied, but for the following experiment in this study, exposures of 0.1 seconds were used.

Method:

1. Set up the MiniPix detector facing upwards, on the lowest floor in the building.
2. Take 4000 frames of data, with each frame set to 0.1s, and record the total number of muons detected.
3. Repeat this twice more, to get a total of three muon counts, which can be totalled.
4. Then change floors, increasing elevation, and repeat the data-taking procedure from the previous step.
5. Total up the amount of muons found on each floor and graph them.

Figure 5 shows the number of muons detected as a function of floor number, with the ground floor being floor 0. This graph showcases a distinct linear relationship between the floor number and the count of detected muons. However, interpreting this outcome as solely due to height sensitivity would be wrong. The variation in muon detection is also attributed to the amount of concrete material present above each floor, influencing the absorption of particles, and acting as an overburden [10]. With increasing floor levels, there is a decrease in the amount of concrete situated above and around the detector's position. This reduction in concrete leads to an increase in muon detection, as less are absorbed before reaching the detector.

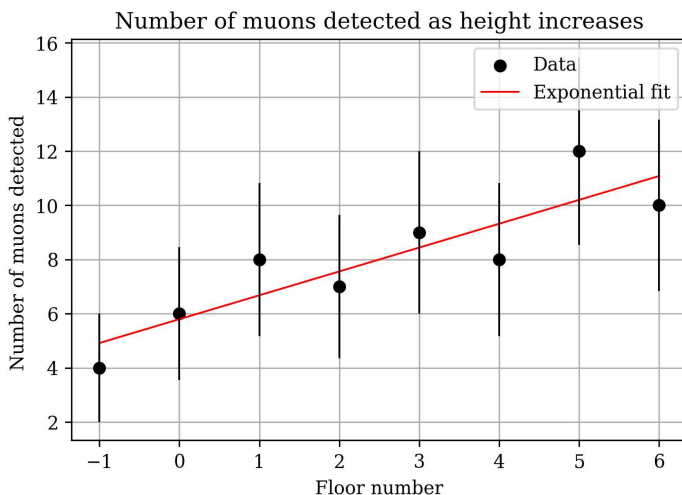


**Figure 5.** Number of muons detected as height increases within the Physics Building at Queen Mary University of London.

Carrying out the second experiment involved travelling to the highest point in London, Hampstead Heath, and setting up the detector at different altitudes to detect muons. An almost identical method was used, by this time instead of floor number intervals, height intervals on the hill were recorded. Figure 6 shows the result of this experiment. Looking at the graph, an exponential function has been fitted to the data collected. The fit yielded a reduced  $\chi^2$  of 0.9696 (to four s.f), which indicates a very good fit.

The fitted model shows the number of detected muons following exponential growth. This outcome aligns with the theoretical expectations, considering that muons are predominantly closer to the upper atmosphere and have very short lifespans [11]. So, it is inferred that a greater number of muons would be found at higher altitudes. The data also follows predictions made by the inverse square law. As the cosmic ray muons can be modelled as originating from a point source, it makes sense that there would be less muons detected closer to Earth surface, and moving higher upward would increase their abundance exponentially. This agrees with the study by Dreesen [12] where they state that "Because muons are created in the upper atmosphere and decay into other particles as they fall to earth, the number detected is greater at higher elevations". Experimenting outdoors strengthens the conclusion that the detector is sensitive to altitude changes of tens of metres.

The uncertainty associated with the count of detected muons follows a square root dependency on the number of observed particles,  $N$ , as the number of observed counts follow a Gaussian distribution. Quantifying the uncertainty on the floor levels in Figure 5 presents a challenge due to the absence of a feasible method for precisely measuring floor heights. For potential future repeats of this experiment, a possible enhancement could involve using an altitude app to acquire accurate floor height measurements in metres, along with their corresponding uncertainties. It is important to note that the experiment's current design is tailored for educational purposes, hence the relatively minor impact of the slight error in the differentiation between floor numbers is negligible.

Furthermore, even in the scenario where each floor's elevation deviated by a few metres, the detector would show little to no discernible difference or a very small marginal one due to the sensitivity limits of the detectors. Consequently, the cumulative error from these discrepancies would be of such insignificance that its consideration becomes unnecessary. In the case of a more sensitive detector, the errors would need to be considered as it would be sensitive enough to detect the differences.

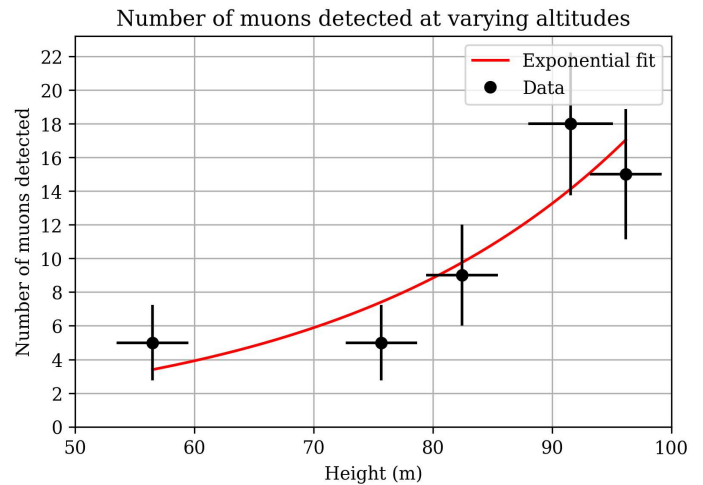


**Figure 6.** Number of muons detected as varying altitudes at Hampstead Heath Hill, London.

Figure 6 resolves the altitude versus overburden issue shown in Figure 5 by demonstrating a distinct correlation between muon detection and height changes, without the presence of concrete. This illustrates the detector's sensitivity to variations in muon counts at different altitudes, which is not caused by overburden. The detector's sensitivity enables it to distinguish particle variations at slight changes in height, which bodes well for students conducting experiments in schools with limited floors and minimal height differences.

With these experiments we can make additional considerations and connections to special relativity. Muons have an extremely short lifetime, with a half-life of only  $15 \mu\text{s}$ ; this means muons live for an average of around  $2.2 \mu\text{s}$ . Without special relativity and travelling at the speed of light, muons should only be able to travel some hundreds of metres. However, cosmic-ray muons can travel from the upper atmosphere to Earth's surface - (tens to hundreds of kilometres). Muons created by collisions in the upper atmosphere have a tremendous amount of energy and travel at approximately 99.995% of the speed of light. When an object travels this close to the speed of light, Einstein's Theory of Special Relativity predicts that effects such as time dilation can occur. These changes depend on the relative motion of the observer and the object so from the rest frame of the muon, the earth and its atmosphere are moving at  $0.99995c$  toward it. This dilation of time, relative to its surroundings, allows the cosmic ray muon to reach the Earth's surface, before decaying into its constituent neutrinos, and either an electron or positron.

### 3.1.2 Variation in Muon Detection with Changing Zenith angle

The highest concentration of cosmic-ray muons incident should be at approximately  $90^\circ$  to Earth's surface (Zenith of  $0^\circ$ ) [13], as that is the most direct route through the Earth's atmosphere to the surface of our planet. Cosmic rays approaching from other angles have a larger distance to cover, so are more likely to be scattered or stopped before reaching the surface. This experiment is designed to find the best angle at which to detect cosmic ray muons.

The experiment had a simple set-up, with the detector fixed in place, and a protractor attached to it. The procedure involved taking a total number of frames for each angle, noting the total amount of muons detected, and then adjusting the detector using the protractor. Only rotations through to  $180^\circ$  were required, but the results would mirror themselves through  $180^\circ$  to  $360^\circ$ .

### Method:

1. Place the detector flat on a table. Make sure the Pixet software is on and ready for data collection.
2. Before changing the angles, record the number of muons detected by the detector when it is flat on the table for 4000 frames.
3. Attach a small piece of Blue Tac to the back of the detector.
4. Carefully position the detector at an angle of approximately 30°. Ensure it is stable and won't fall.
5. Allow the detector to record the number of muons for 4000 frames, keeping the setting the same as before.
6. Record the number of muons and the angle.
7. Repeat the above steps for angles of 60°, 90°, 120°, 150°, and 180° (facing the floor). Make sure to adjust the angle of the protractor such that it stays upright/ that you can read the angle which the detector is at.
8. For each angle, record the number of muons detected.

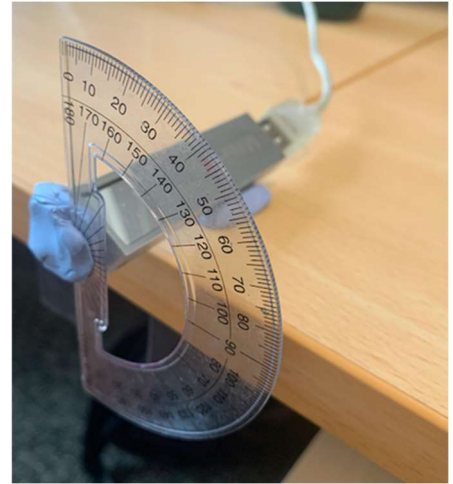


**Figure 7.** Image of the experimental set up for exploring the best angle to place the detector for maximum muon detection.

The graph of these results is plotted in Figure 8. The number of detected muons is higher between 30° to 150° compared to 0° and 180°. This finding seems odd but can be explained logically: muons are much more likely to travel straight downwards. When muons travel straight down from the sky, they are less likely to be detected as distinct muon tracks and appear as dots on the detector. When particles strike the detector, they deposit energy to the pixels, which are then highlighted by the screen. If a muon hits the detector travelling straight downwards, then the track it leaves behind will only be a small spot. However, when muons approach at an angle, their path length through the detector's sensitive region becomes more distinguishable, giving the result of the best angle to measure muons being around 40°. This peak is shown in Figure 8. It should be noted however, that Figure 8 only displays the upper bound of the statistical uncertainty on the count. There is an additional caveat to this experiment which is it was conducted indoors, but near a window, so the amount of muons reaching the detector is also influenced by the concrete of the above floor in the building.

Expanding on Section 4.5, the MiniPix detector's software, Pixet, uses an algorithm to recognise identifiable particle tracks. At the angle of 40°, cosmic ray muons travelling orthogonally to Earth's surface will strike the detector and create more tracks, making it easier for the Pixet software detection algorithms to identify them as muons. At a rotated angle of approximately 90°, there is a small decrease in total counted muons, as the detector is now parallel to a large amount of incoming cosmic ray muons; this increases the likelihood that these particles will miss the detector entirely.

The error shown highlighted in the graph is a combination of both angular measuring and counting errors. In truth, while the peak of muons appears to sit at approximately 30 (±) 5°, it is in fact at 0°, but this is most detectable around 30 (±) 5°.

The error in Figure 8 stems from a few areas. The first is on the angle and the second is the error on the number of muons detected. The error on the angle is a human error, identified to be (±) 1°, and the error on the number of muons is the same as before, with the square root of each value of muons detected. The error from the window means that more muons will appear from that side. However, it is such a marginal difference that it has very minimal effect. This error is represented in Figure 8 by the opaque pale blue rim on the edge of the plot.

This experiment is useful in two ways for outreach, its results are both informative about the nature of cosmic ray muons but also require an analytic approach to technological limitations in making scientific measurements.

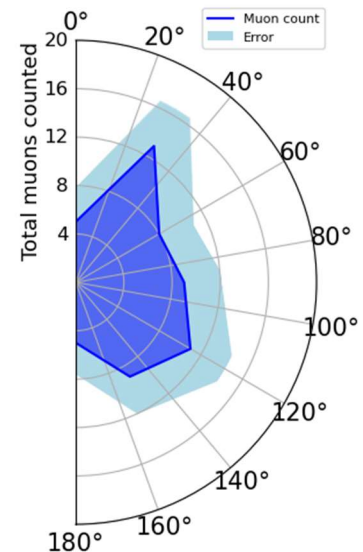


**Figure 8.** A graphical representation displaying the best angle to place the detector for maximum muon detection.

### 3.2 Source Radiation Experiments

The following experiments each involved the use of a radioactive source. For each experiment, the source in question was a thoriated rod, which was observed to produce primarily alpha radiation, and secondarily beta radiation. This made the rod a versatile source, useful for a variety of experiments. Thorium will eventually decay into lead, a stable element via several alpha and beta decays, making it a perfect low risk source for the following experiments for GCSE students [14].

#### 3.2.1 Velocity and Kinetic Energy Analysis in Beta Decay

The detection capabilities of the “MiniPix EDU” detectors go beyond the study of muons; in this section the velocities of electrons involved in beta decay experiments are investigated. This experiment was inspired by the ADMIRA project which aims to enable students at secondary schools to understand Particle Physics and experience the latest technology in cosmic radiation imaging [15].

Method:

1. Set up the MiniPix detector and run it until at least five electrons (beta particles) are visible on the detector screen. Start with around 4000 frames.
2. Identify five electrons (beta decays) on the detector screen. It is possible to use a radiation source to find faster electrons, but this is not a necessity.
3. Zoom in on each of these electrons on the detector screen so that all the pixels representing an individual electron are visible (like the images of the particles on page 8).
4. Under the ‘Image Info’ tab on the Pixet software GUI, take note of the value labelled 'total'. This is the kinetic energy of the electron in keV (or kiloelectron volts).
5. Convert each electron's kinetic energy from keV to Joules by dividing the kinetic energy by  $6.2415 \times 10^{15}$ . Now the energy is in Joules.
6. Using the equations and values given below, sub in the values and the kinetic energy found to get the speed  $v$ :

a. Classical Kinetic Energy  $\rightarrow v = \sqrt{\frac{2E_k}{m}}$  (1)

b. Relativistic Kinetic Energy  $\rightarrow v = c \sqrt{1 - \frac{1}{1 + \frac{E_k}{E_0}}^2}$  (2)

Where  $E_k$  is kinetic energy,  $c$  is speed of light, and  $m_0$  is rest mass of electron

7. Repeat this for all the electrons identified.
8. Repeat all above steps but this time find 5 alpha particles, and use the mass of a helium nucleus.

Figure 9 shows the results of this experiment using electrons, the orange histograms represented the velocity calculated using the relativistic formula and the blue histograms show the velocity calculated with the classical formula. This graph shows the need for relativity compared to using classical mechanics. Most of the blue bars cross over the red dotted line (speed of light), which students will know is impossible. As these particles cannot physically travel faster than the speed of light [16], equation (2) must be used, not equation (1). Therefore, this is a great and easy visual experiment for GCSE students to do to understand the importance of relativity for particles at high speeds.

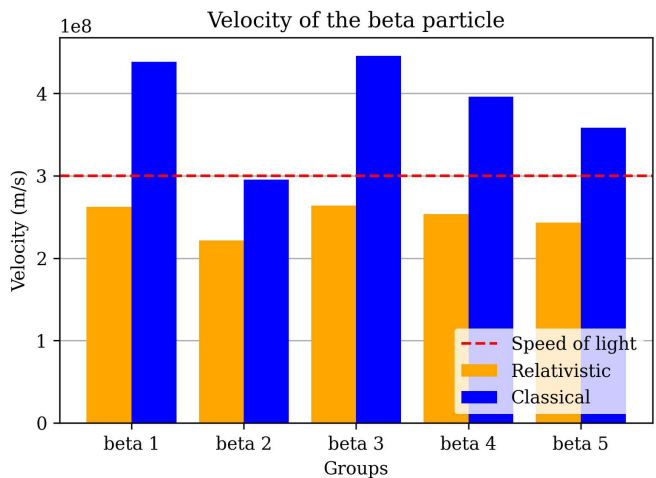


**Figure 9.** Comparing the relativistic formula to the classical formula on beta particles to see the difference in velocity.

The data presented in Figure 10 demonstrates the inadequacy of classical mechanics in describing the behaviour of particles at velocities close to the speed of light. In contrast, experiments involving alpha particles yielded the same velocity for classical and relativistic speeds, with both values being  $\frac{1}{3}$  to  $\frac{1}{2}$  of the speed of light. Although these velocities only remain below the speed of light by a single order of magnitude, this shows that the particle must be very close to the speed of light before there is a requirement for relativistic considerations.

In the classical limit (objects larger than submicroscopic and moving slower than about 1% of the speed of light), relativistic mechanics becomes the same as classical mechanics [17]. This agrees with the data found, showing that the difference was only noticeable for particles very close to the speed of light,

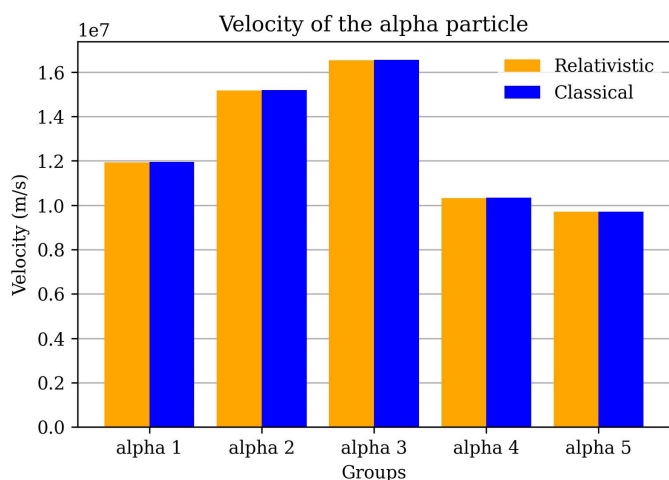


**Figure 10.** Comparing the relativistic formula to the classical formula on alpha particles to see the difference in velocity.

and not for alpha particles, as seen in Figures 9 and 10.

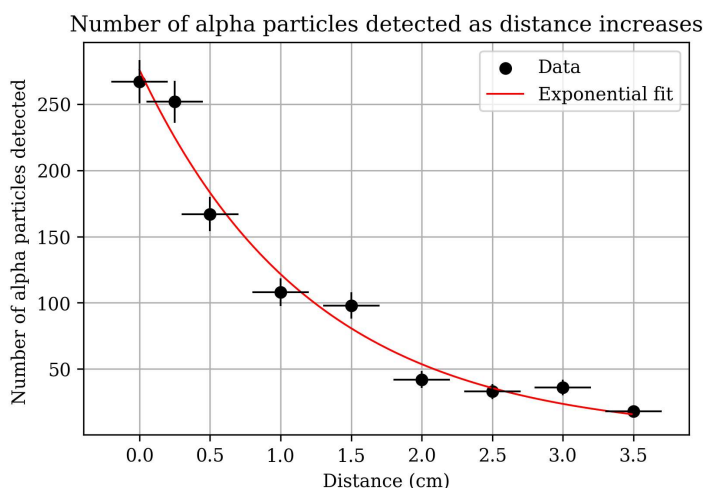
Comparing the two velocity values from each particle, the errors attributed to the individual measurements can be dismissed. Since both values are subject to similar levels of uncertainty, these errors are considered inconsequential for the purpose of the comparison. The focus of this experiment was solely on the comparative analysis between the two values.

### 3.2.2 Decay Characteristics of Alpha Radiation as a Function of Distance

Investigating the interaction of alpha particles with air provides essential insights into their energy attenuation. This experiment, though straightforward in nature, yields great results, thanks to the easily observable inverse square law, providing a striking exponential decay. By setting up an alpha source at various distances away from the detector, the number of alpha particles at each distance can be recorded.

Method:

1. Set up the radiation detector with the radioactive alpha source placed at 0 cm from the detector screen, though making sure not to make actual contact with the screen.
2. Run the detector for 2000 frames and count the number of alpha particles that appear on the screen during this time.
3. Move the radioactive alpha source to a distance of 1 cm from the detector screen.
4. Repeat step 2, running the detector for 2000 frames and counting the number of alpha particles.
5. Continue moving the radioactive alpha source away from the detector in 1 cm intervals (or 0.5cm intervals if time permits) until a distance of 5cm is reached, repeating step 2 at each distance.
6. Record the distance from the source to the detector and the corresponding number of alpha particles detected in a data table.



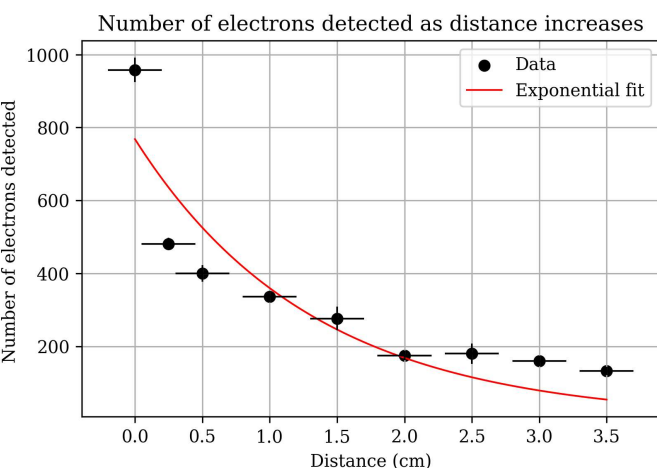
**Figure 11.** The number of alpha particles detected as the distance from the thoriated rod increases.

Figure 11 shows the number of alpha particles detected as a function of distance from the rod. The graph shows an exponential decay fit, which fits the predictions made by the inverse square law for radiation. The reduced  $\chi^2$  from Figure 11 is found to be 1.2. This implies that the fit is good.

The initial segment of the graph demonstrates a rapid decline in alpha particle counts over the first few centimetres. By the 3 cm mark, a large diminishment in these alpha particles is observed, signifying the substantial attenuation by the air. This experiment is a clear demonstration of the inverse square law [18]. Present throughout many areas of Physics, GCSE students may be familiar with the concept, but may not have been taught the theory behind the inverse square law directly. This experiment provides a hands-on experience observing the effects of both the inverse square law and the attenuation of alpha radiation by air.

In Figure 11, the exponential decay has an equation of  $y = 274e^{-0.83x}$ .

Figure 12 shows the number of detected electrons as a function of distance from the rod. The electrons in Figure 12 do not follow the same exponential decay pattern. This has been put down to neutrinos carry away a percentage of the energy from the detector, and this percentage changes for every decay. Neutrinos are not



**Figure 12.** The number of electrons detected as the distance from the thoriated rod increases.

detected by the detector, so this leads to the discrepancy in the electron data vs the alpha data. If it was possible to measure both electrons and neutrinos, then the exponential decay trend would be the same.

The uncertainty in the distance measurement stems from human error, which is estimated to be approximately 2 mm. Regarding the alpha particle count, the associated error is determined by taking the square root of the recorded count of alpha particles.

### 3.2.3 Material Attenuation with Alpha Particles

The objective of this experiment was to assess the attenuation of alpha particles as they traverse different materials. Specifically, it focuses on quantifying the reduction in alpha particle count when different materials are placed between the particle source and the detector.

Method:

1. Ensure a safe and controlled environment for the experiment.
2. Keep the radiation source at a distance of 0.5 cm away from the detector.
3. Take 4000 frames of data with the radiation source at 0.5 cm away.
4. Record the number of alpha particles detected on the detector.
5. Now test how well materials shield the alpha from the detector by placing different materials between the detector and the radiation source.
6. Take 4000 frames of data for each material that you used, and record the number of alpha particles detected. Start with the thinnest material and finish with the thickest.

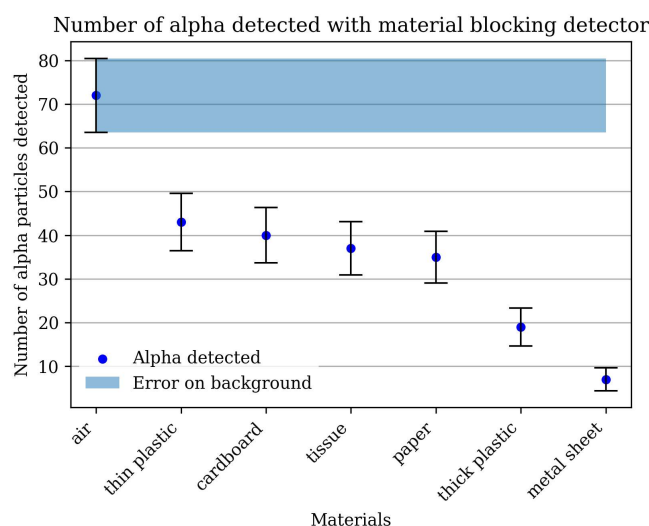


**Figure 13.** The amount of radiation detected when different materials block the detector from the thoriated rod.

The graphical representation in Figure 13 shows the relationship between materials and the degree of alpha particle penetration. As seen previously, air demonstrates a certain threshold, approximately 3.5 cm, beyond which it effectively stops alpha particles [19], as shown in Figure 13. This effect is further accentuated when objects are placed in the particle path. The efficacy of attenuation scales proportionally with the thickness of the intervening object. As the thickness increases, the amount of alpha detected decreases. Among the array of materials tested, metal emerges as the most effective in stopping alpha radiation, displaying the highest degree of particle containment.



However, even materials as thin as tissue can result in a nearly 50% reduction in alpha particles recorded by the detector.

The uncertainty in the error shown in Figure 13 comes from multiple variables, including material thickness and density. This error comes from the square root of the total number of alpha particles detected, which originates from the assumption that the number of counts follows a Gaussian distribution.

#### 4. Discussion

This section will discuss what the results of these five experiments teach us about the detector's capabilities to successfully detect particles, as well as the limitations found. This includes how the detectors can be used in a secondary school environment.

##### 4.1 Insights Gained from the Detector Analysis

The collective outcomes of these experiments provide us with a comprehensive insight into the MiniPix detector's capabilities. Through these investigations, a good understanding of the detector's sensitivity has been gained, which has proven to be much higher than the initial thoughts. It was thought that the detectors would be able to distinguish between the particles, but not have any difference with the height, but this was disputed by several of the experiments undertaken. The detector is able to easily distinguish between particle type, as shown in Figure 3, and reliably counts them in their particle groups. It measures the kinetic energy, allowing the velocity of the particle to be found, and it also showcases the direction of particles, allowing for the best angle and place to detect particles. It showcases an ability to discern variations in muon counts even between floors on a building. The accuracy and success of the alpha distance experiment shows the detector's accuracy and affirm its functionality as intended.

Knowing all of this, a first collection of GCSE-level experiments has been devised, but many more can be used too.

##### 4.2 Detector limitations

However, certain limitations are worth acknowledging. The detector's thin and flat surface introduces a constraint: particles that enter vertically tend to register as dots rather than as traceable paths. This means that not all particles will be detected. A perfect scenario would involve placing detectors in a circular arrangement, enabling particles to be counted from several directions rather than from a single plane, and yielding more accurate results. If the detector was composed of thicker material, orthogonal incident particles would still register as tracks, instead of dots. The detector cannot detect outside in direct sunlight as it overloads the pixels, causing an energy dump too high to detect anything from. It can also be easily damaged, as seen with the thoriated rod getting too close to the surface of the detector.

The detector proves highly effective for studying alpha decay and muons, demonstrating its remarkable capabilities in these domains. But its performance in investigating beta decay has limitations due to the presence of neutrinos accompanying the electrons, which carry away a percentage of the energy from the detector. However, the fact that we can see an energy difference from neutrinos adds to the conclusion that the detector is sensitive enough to distinguish between many particles.

Another limitation arose when excessive energy from direct contact with alpha particles damaged the detector surface. Bringing the thoriated rod very close to the detector screen caused a substantial energy transfer, resulting in pixel damage. Identifying this issue was crucial, as it highlighted the necessity of maintaining a safe distance between the alpha rod and the detector screen to prevent pixel burnout. This limitation has more significance, as it restricts the detection of particles from the thoriated rod at extremely close distances to the detector.

The detector's incapacity to function in direct sunlight becomes apparent as a notable constraint. In this instance, excessive energy deposition renders the detector non-operational. Yet, a simple fix, such as employing an umbrella to shield the detector from direct sunlight, restores its full functionality without damage to the detector. This circumstance underscores a fundamental restriction in the detector's energy absorption capacity, with direct sunlight exceeding this threshold.

There are also several places in which errors can occur. The error in distance measurements stems from the subjectivity of human visual assessment. The uncertainty associated with particle counts adheres to the consistent rule that the error corresponds to the square root of the detected particle count.

Moreover, the detector lacks the necessary sensitivity to differentiate between materials, as depicted in Figure 13. Even though materials like thin plastic, cardboard, tissue, and paper possess distinct characteristics, they exhibit similar levels of alpha penetration. This indicates that the detector can detect thickness differences, but falls short in distinguishing specific materials.

### 4.3 Outreach applications

Now that all the experiments have been carried out, and the sensitivity and detecting capabilities of these detectors have been explored, they can be written up with secondary school students in mind. This provides the opportunity to share information about the optimal detector placements, suggest the most effective experiments to enhance the detector's capabilities and offer guidance on the ideal angle for students to position the detector.

These experiments collectively serve as engaging educational tools that enable secondary school students to explore fundamental concepts in Particle Physics and experimental methodologies. By providing a connection between theoretical concepts and real-world observations, these experiments give an appreciation for the intricate nature of the physical world. Furthermore, these hands-on experiences instil critical thinking skills, encouraging students to question, analyse, and draw conclusions from empirical data.

The outreach applications extend beyond textbook learning, hopefully inspiring students to consider scientific concepts from a practical standpoint. Engaging with particle detectors and conducting experiments equips students with foundational skills in experiments, data collection, and analysis – skills that are invaluable in the scientific world. Moreover, these experiments ignite curiosity, sparking a passion for Physics and science and providing a gateway to exploring advanced topics in Physics.

## 5. Conclusion

In conclusion, the MiniPix EDU particle detector proves to be an excellent educational tool, especially for catering to the learning needs of secondary school students. By immersing students in the realm of particle interactions and fundamental Physics Principles, this device significantly enriches their GCSE education journey. The hands-on approach facilitates active learning and holds the potential to start a passion for scientific discovery.

While certain limitations, such as its susceptibility to direct sunlight and its flat detector surface, do exist, these constraints bear minimal relevance to the fundamental learning objectives targeted at the GCSE level. Notably, the detector adequately captures an array of particles, thereby allowing students to undertake practical experiments and attain insights into the world of Physics.

Looking ahead, there are some avenues for refining the device's functionality. Enhancements to the software, particularly the implementation of mechanisms to mask malfunctioning pixels from the display, would be of significant benefit. Furthermore, an effective cooling mechanism for the detector holds the potential to extend its operational duration, opening avenues for prolonged experimentation, and therefore reduction in statistical uncertainty of the measurements performed.

## Acknowledgments

The authors would like to thank the South East Physics Network (SEPnet) for offering us the invaluable opportunity to undertake this project and for providing the funding. We would like to thank the Particle Physics Research Centre at Queen Mary University of London for hosting this project and giving us a taste of particle physics research. We really appreciate the guidance and support from the rest of the Particle Physics Research Centre team at Queen Mary University of London throughout the course of this project. Special thanks go to Dr Abbey Waldron for her exceptional assistance and contributions throughout. Dr Booth and Dr Cremonesi would like to thank the Queen Mary university of London Centre for Public Engagement for funding the purchase of the equipment.

## References

- [1] ADVACAM MiniPIX EDU, Portable USB Camera for Education, Accessed 16/08/23, <https://advacam.com/camera/minipix-edu>
- [2] S. Jackson NASA, CERN Timepix Technology Advances Miniaturised Radiation Detection, Oct 4, (2019), accessed 16/08/23 <https://www.nasa.gov/feature/nasa-cern-timepix-technology-advances-miniaturized-radiation-detection>
- [3] The Centre for Public Engagement, About Public engagement, Public Engagement, Queen Mary University of London, accessed 22/08/23, <https://www.qmul.ac.uk/publicengagement/about-engagement/centre-for-public-engagement/>
- [4] Archer, Martin O. "Schools of all backgrounds can do physics research—on the accessibility and equity of the Physics Research in School Environments (PRiSE) approach to independent research projects." *Geoscience Communication* 4, no. 2 (2021): 189–208. Accessed 22/08/23 <https://gc.copernicus.org/articles/4/189/2021/>
- [5] Outreach Team, “MINIPIX EDU Students’ Manual” draft, Particle Physics Research Centre, Queen mary University of London, Page 7 “Working Principles’, accessed 17/8/13
- [6] User:SyntaxError55, “File:Atmospheric Collision.svg”, WIKIPEDIA Commons 27/10/2007, Accessed 1/8/2023, [https://commons.wikimedia.org/wiki/File:Atmospheric\\_Collision.svg](https://commons.wikimedia.org/wiki/File:Atmospheric_Collision.svg)
- [7] Llopert X 2007 Design and characterization of 64K pixels chips working in single photon processing mode *PhD Thesis*(Accessed 22/8/23), <http://cds.cern.ch/record/1056683?ln=ca>
- [8] Llopert X, Ballabriga R, Campbell M, Tlustos L and Wong W 2007 Timepix, a 65k programmable pixel readout chip for arrival time, energy and/or photon counting measurements *Nucl. Instrum. Methods Phys. Res. A* 581 485–94 , accessed 22/8/23, <https://www.sciencedirect.com/science/article/pii/S0168900207017020?pes=vor>
- [9] Campbell M 2001 Electronics for pixel detectors *7th Workshop on Electronics for LHC Experiments* (CERN Document Server) 11–16, <https://iopscience.iop.org/article/10.1088/1361-6552/ac4143/meta>
- [10] J. Bramante, “Dark matter, detection, an overview of overburdens”, Queen’s University, The McDonald Canadian Astroparticle Physics Research Institute, Perimeter Institute, accessed 16/8/23, <https://indico.cern.ch/event/1027519/contributions/4325877/attachments/2244424/3806019/DM%20Detection%20Overburdens.pdf>
- [11] B. Armbruster, I. M. Blair, B. A. Bodmann, N. E. Booth, G. Drexlin, J. A. Edgington, C. Eichner et al. "Upper limits for neutrino oscillations  $\nu^- \mu^- \rightarrow \nu^- e^-$  from muon decay at rest." *Physical Review D* 65, no. 11, 1-16 (2002)
- [12] K. Dreessen, Seeing the Invisible, GENESOCENE, Nov 16, pp. 1 (2020), accessed 14/08/23, <https://scene.geneseo.edu/2020/11/seeing-the-invisible/>
- [13] M. Bektasoglu, H. Arslan, “Investigation of the zenith angle dependence of cosmic-ray muons at sea level”, *Pramana Journal of physics*, c Indian Academy of Sciences , Vol. 80, No. 5, ( May 2013), Page 843, accessed 16/8/23, <https://www.ias.ac.in/public/Volumes/pram/080/05/0837-0846.pdf>
- [14] Olley, Jon M., Andrew Murray, and Richard G. Roberts. "The effects of disequilibria in the uranium and thorium decay chains on burial dose rates in fluvial sediments." *Quaternary Science Reviews* 15, no. 7 (1996): 751-760
- [15] R. Ballabriga, A. Le Gall, 29 March, 2021, “TimePix-based detectors bring particle physics in the classroom”, CERN knowledge transfer, Accessed 16/8/23 <https://kt.cern/news/news/knowledge-sharing/timepix-based-detectors-bring-particle-physics-classroom>
- [16] G. Feinberg, (February 1970), “Particles That Go Faster Than Light”, *Scientific American* Vol 222, No.2, page 69, accessed 16/8/23 [https://www.jstor.org/stable/24964494?searchText=%28Particles+that+go+faster+than+light%29&searchUri=%2Faction%2FdoAdvancedSearch%3Fq0%3Dparticles%2Bthat%2Bgo%2Bfaster%2Bthan%2Blight%26f0%3Dall%26c1%3DAND%26f1%3Dall%26acc%3Don&ab\\_segments=0%2Fbasic\\_search\\_gsv%2Fcontrol&refreqid=fastly-default%3A67393335a5b35e23078bd192a4617140](https://www.jstor.org/stable/24964494?searchText=%28Particles+that+go+faster+than+light%29&searchUri=%2Faction%2FdoAdvancedSearch%3Fq0%3Dparticles%2Bthat%2Bgo%2Bfaster%2Bthan%2Blight%26f0%3Dall%26c1%3DAND%26f1%3Dall%26acc%3Don&ab_segments=0%2Fbasic_search_gsv%2Fcontrol&refreqid=fastly-default%3A67393335a5b35e23078bd192a4617140)
- [17] P. P. Urone, R. Hinrichs, (2023), *Special Relativity*, LibreTexts Physics, Ch 13, 571-588, accessed 14/08/23
- [18] N.s Voudoukis, S. Oikonomidis, (November 2017), “Inverse Square Law for Light and Radiation: A Unifying Educational Approach”, *EJERS, European Journal of Engineering Research and Science* Vol.2, No.11.,Page 23, I. Introduction, accessed 16/8/23 <https://ej-eng.org/index.php/ejeng/article/view/517/212>
- [19] arpana, “Alpha Particles”, “What are the properties of alpha particles?”, Australian government, Australian radiation Protection And Nuclear Safety Agency, accessed 16/8/23 <https://www.arpana.gov.au/understanding-radiation/what-is-radiation/ionising-radiation/alpha-particles>